

OPTIMIZATION OF EFFICIENCY, REGULATION AND SPECIFIC ABSORPTION RATE OF A TRANSCUTANEOUS ENERGY TRANSMITTER WITH RESONANT CAPACITOR

Daniela Wolter Ferreira and Luiz Lebensztajn

*Laboratório de Eletromagnetismo Aplicado, Escola Politécnica da Universidade de São Paulo,
Av. Prof. Luciano Gualberto, Travessa 3, 158, Cidade Universitária, São Paulo, Brazil*

Keywords: Specific absorption rate, Induced current density, Transcutaneous energy transmitter, Resonant capacitor.

Abstract: The induced current density and Specific Absorption Rate (SAR) in the skin around a Transcutaneous Energy Transmitter (TET) was analyzed. The considered TET was projected with serial resonant capacitor and had its efficiency, regulation and SAR optimized by a multi-objective genetic algorithm (MGA), considering a range of TET parameters. A surrogate approach (Kriging) was also used to model the objective functions and support the optimization with less computational cost.

1 INTRODUCTION

The main problem of the artificial organs mostly or completely implanted inside the body is the power supply. For this reason, several researchers (Dissanavake et al., 2009, Joung and Cho, 1996 and Ghahary and Cho, 1992) have studied a way to transfer electric energy to the internal artificial devices without the need for direct electrical connectivity, thus decreasing the chances of infections, allowing more comfort and offering more flexibility to the patient's daily activities. This is called Transcutaneous Energy Transmission technology, or TET, and it is normally achieved by means of electromagnetic fields, similar to a transformer with skin between primary and secondary windings. This however, creates high values of regulation, low coupling and considerable induced currents, requiring higher voltage from the battery at low efficiency.

In order to increase the efficiency and decrease the regulation, some researchers such as Joung and Cho, (1996) and Ghahary and Cho (1992) use resonant capacitors to compensate the leakage inductance of the windings of the TET.

This paper studies the behavior of the induced current density and Specific Absorption Rate (SAR), proposed by Johson (1975), generated by a TET with associated series resonant capacitors that was projected to optimize efficiency, regulation and SAR

by changing the frequency, core geometry and wire turns while maintaining the necessary power to the artificial organ.

In order to simulate the magnetic effects, a finite element method software (Flux-2D) was used with several different configurations to generate a set of data, which was then used by a Kriging model (Lebensztajn et al., 2004) to perform data interpolation.

2 PRINCIPLES

Fundamentally, the TET has one external part (transmission system) and one subcutaneous internal part (receiving system) as shown in Figure 1.

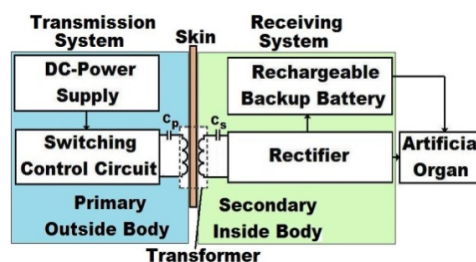


Figure 1: TET's block diagram.

The TET works as a very thin transformer in which the process of transmission is composed of an external battery connected to the input of an

oscillation circuit that transforms the DC voltage to high frequency AC voltage at the output to which an external coil (primary) is connected. The receiving system has an internal coil (secondary) that receives the alternating magnetic field and transforms it to AC voltage. A rectifier circuit is then used to supply DC power to the artificial organ and the internal backup battery. In this paper, capacitors, calculated to compensate the leakage inductance of the primary and secondary coils, are connected in series to each winding. The geometry of the transformer is optimized in a cylindrical shape of ferrite cores and copper coils as shown in Figure 2.

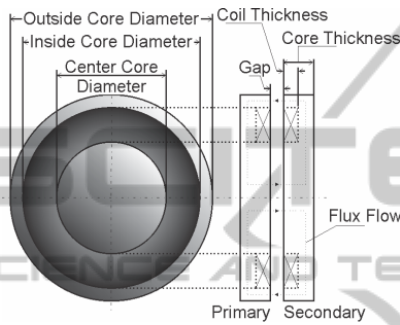


Figure 2: Geometry of the considered transformer - Top and Cross View.

This geometry was simulated in Flux-2D with different configurations keeping some parameters fixed while varying other parameters as depicted in Table 1.

Table 1: Design parameters of the transformer.

Parameters		Values
Fixed	Gap between primary and secondary	5 mm
	Core Thickness	5 mm
	Outside Core Diameter	50 mm
	Inside Core Diameter	40 mm
Variable	Center Core Diameter	[8 24] mm
	Coil Thickness	[1 4] mm
	Primary wire Turns	[23 45] mm
	Secondary wire Turns	[23 45] mm
	Source Voltage	[16 30] V
	Frequency	[100 300] kHz

As this geometry can be modelled by the transformer's complete model, capacitors were added in series with the primary and secondary windings to compensate the leakage inductance. In this way, those capacitors could be calculated by:

$$C=1/\omega^2.L_d \quad (1)$$

In this equation, $\omega=2.\pi.f$, whereas f is the considered frequency and L_d is the leakage inductance of the considered configuration.

2.1 Optimization

A multi-objective genetic algorithm (MGA) method was used with three different objective functions:

1. Maximize efficiency.
2. Minimize regulation.
3. Minimize SAR.

In addition, two kinds of constraints were considered:

1. The load power is greater than a specified value.
2. The reserved areas for the coils have enough space for the number of wire turns.

As a typical multi model optimization, the MGA solution cannot be improved with respect to any objective function without worsening at least one other objective function. Hence, a set with more than one optimal solution, which differs from each other by the evaluation of each objective function, can be found. This means that each configuration cannot be dominated by any other on the set and thus it is called non-dominated set.

However, it is too time consuming for the MGA to run a new simulation in Flux-2D for every new configuration that the optimization requests for achieving the better data. Hence, in order to support the optimization method with less computational cost, the Universal Kriging (Lebensztajn et al., 2004) was employed to create a model which could be used by MGA at any moment without the need of simulating a new configuration in Flux-2D.

The Kriging uses: 1) a set of polynomials ($p(x)$) which is intended to follow the general tendency of the function to be modelled, and 2) a set of Gaussians ($h(x)$) that makes it possible to follow the fluctuations around the general tendency. Therefore, the model can be written by:

$$y(x) = w^T.h(x) + c^T.p(x) \quad (2)$$

w^T and c^T are the weights for each Gaussian and polynomial respectively, which could be determined through the set of data. The Universal Kriging assumes that a trend ($c^T p(x)$) can be written as a linear combination of known functions, determined by the physics of the problem being dealt with and is performed by a second-order polynomial (full quadratic model, for example). Subsequently, the stochastic portion of (2) ($w^T h(x)$) was calculated.

3 METHODOLOGY

3.1 The TET and its Electromagnetic Effects on Biological Tissues

In Flux-2D, the transformer was designed with the core geometry shown in Figure 2. The properties of the materials utilized in this software to construct this geometry were the properties of ferrite for the cores and copper for the coils, as well as the wet skin electrical properties (electrical conductivity and the relative permittivity) as defined by the Institute for Applied Physics Nello Carrara, even considering the differences for each simulated frequency of Table 1.

Moreover, utilizing the electrical circuit and magnetic geometry coupling capability of this software, the DC-power supply and switching control circuit were implemented as a sinusoidal AC power source. The receiving system after the internal coil (rectifier and other blocks shown on the secondary of Figure 1) was simulated through a load resistance that absorbs at least 12 W.

Virtual short and open circuit tests were also performed by running the software with resistance value $10^{-10} \Omega$ and $10^{+10} \Omega$, respectively. After these tests were conducted with each of the configurations of Table 1, electric current, voltage and power were collected on the primary and secondary circuit, allowing the attainment of the complete model of the transformer and, subsequently, the series resonant capacitors as mentioned on equation 1.

Thus, all the configurations were again simulated with the series resonant capacitor as shown in Figure 1, collecting once more the electric current, voltage and power in the load and in the sinusoidal power source to calculate the efficiency and regulation from the source to the load, and the SAR and induced current density in the skin.

3.2 Optimization

From the last simulations executed with all the configurations shown on Table 1 while using serial resonant capacitors, a pool of data was collected for the use by the surrogate approach (Kriging model).

Results from random configurations from this pool data was chosen and inserted into *RSTool* from Matlab to obtain a full quadratic model for the efficiency, regulation, SAR, and load power, represented by c^T and $p(x)$ of equation 2. Since six variables were used (the variable data on Table 1) to create each model, the polynomials of equation 2 are written by a constant term, six linear terms, 15

interaction terms (pair-wise products of the variables), and six squared terms of each variable. The weight c of each term is the vector of coefficients calculated by *RSTool*.

In addition, the residuals from *RSTool* were used to obtain the Gaussian tendency parameters, w^T and $h(x)$. This means that the coefficients of w were evaluated by using maximum likelihood estimation as described in Lebensztajn et al. (2004) on the set of residuals.

In order to ascertain the attained model, the efficiency, regulation, SAR, and load power were estimated through this pattern for all the simulated configurations and compared with the other values in the data pool, as shown in Figure 3, resulting in errors smaller than 15 %. This means that the Kriging model is consistent and can be used to support the objective function in the optimization process.

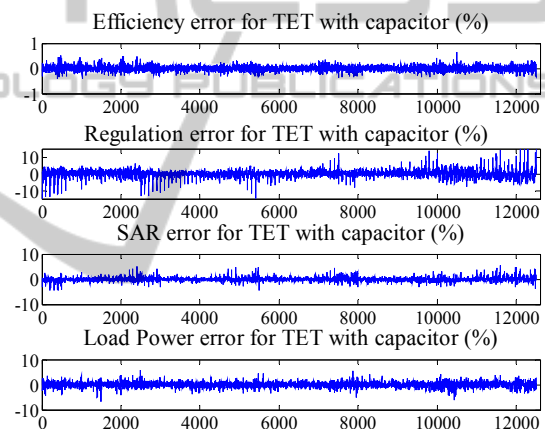


Figure 3: Percentual error of the kriging model compared to the simulation with Flux-2D for efficiency, regulation, SAR and load power. Each point on x axis means each configuration combining parameters according to Table 1.

Hence, the MGA technique of *optmintool* from Matlab was applied to maximize the efficiency while minimizing regulation and SAR, considering the mentioned constraints, which were implemented as penalty functions as in Vieira et al. (2004).

4 RESULTS

The MGA resulted in a set of 32 different configurations (the non-dominated set), which were simulated again by Flux-2D.

Figure 4 presents the value of efficiency, regulation, and SAR obtained from the Kriging model and the Flux software, indicating that the

Kriging model has very good reliability.

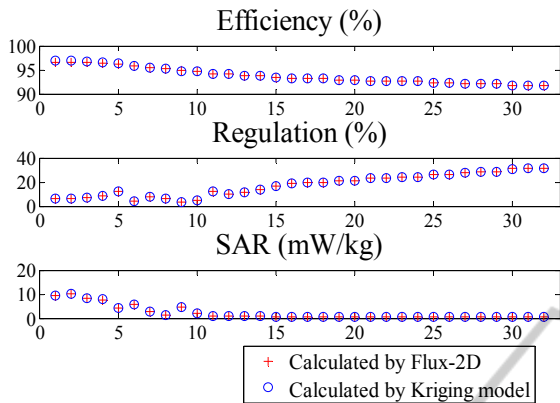


Figure 4: SAR, efficiency and regulation - Comparison between data calculated in Flux-2D and estimated from Kriging model. Each point on x axis means each configuration on the non-dominated set, selected by MGA.

Figure 5 shows that, from all the configurations chosen by MGA, the worst value of SAR is also the highest value of the maximum current density, e.g., 10.2 mW/kg and 1.8 A/m². However, the worst current density compared to the limit of ICNIRP was 0.83 A/m² at 107.3 kHz, which is equal to 77 % of the maximum current density for this frequency. For all other configurations, the current density is always lower than 77 % of the maximum current density (ICNIRP, 1998).

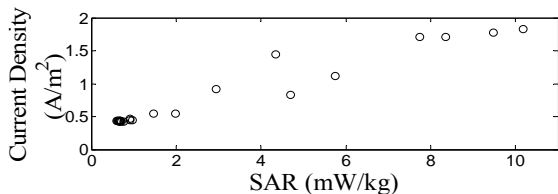


Figure 5: Values of maximum current density and SAR for each configuration resulted from MGA.

From Figures 4 and 5, the efficiency improves together with regulation (efficiency increase as regulation decreases) and the SAR improves together with the induced current density (both decreases together), but each pair improves with the depreciation of the other. This behaviour can also be seen on Table 2, which also shows that all chosen configurations are possible to be constructed mechanically. The induced values of SAR and current density are also within the limits proposed by ICNIRP (1998), i.e., 10 W/kg and frequency divided by 100, respectively.

Table 2: Selected configurations from MGA and results.

Configurations						Results			
Frequency [kHz]	Primary Wire Turns	Secondary Wire Turns	Voltage [V]	Center Core Diameter [mm]	Coil Thickness [mm]	Efficiency [%]	Regulation [%]	SAR [mW/m ²]	Induced Current Density [A/m ²]
289.1	5	23	29.99	8.10	2.27	96.7	6.4	9.49	1.77
284.8	43	23	29.91	8.24	2.22	96.6	6.3	10.17	1.83
279.6	44	23	29.81	10.99	2.27	96.5	7.1	8.35	1.71
277.2	43	23	29.70	13.05	2.43	96.4	8.2	7.74	1.71
277.9	45	23	26.88	18.66	2.36	96.3	12.3	4.34	1.44
161.2	44	24	27.79	8.26	2.31	95.9	4.4	5.75	1.11
153.7	38	24	23.53	19.11	2.68	95.5	7.8	2.94	0.92
111.4	38	24	19.20	19.05	2.83	95.2	6.1	1.46	0.54
107.3	44	23	29.93	8.13	2.22	94.8	3.3	4.69	0.83
104.2	44	28	20.45	9.59	2.32	94.7	5.0	1.98	0.54
108.2	45	30	19.55	21.38	2.94	94.2	12.1	0.92	0.47
104.5	44	31	18.03	18.07	2.93	94.1	9.9	0.97	0.45
103.1	44	32	18.05	18.93	3.06	93.9	11.6	0.91	0.44
101.5	44	31	18.56	22.47	2.87	93.8	13.5	0.77	0.43
101.5	44	33	17.95	22.44	3.01	93.3	16.6	0.71	0.43
101.4	44	33	18.42	23.55	2.98	93.2	18.6	0.70	0.43
100.9	44	33	18.38	23.64	3.16	93.2	19.3	0.68	0.43
101.2	44	33	18.33	23.77	3.10	93.2	19.5	0.67	0.43
101.0	44	34	18.10	23.55	3.17	92.9	20.9	0.67	0.43
101.1	44	34	18.07	23.60	3.18	92.9	21.3	0.66	0.43
100.9	44	35	17.97	23.72	3.18	92.7	23.3	0.65	0.43
100.8	44	35	17.94	23.73	3.19	92.7	23.5	0.64	0.43
100.9	44	35	17.96	23.81	3.23	92.7	24.0	0.64	0.43
101.0	44	35	17.93	23.84	3.22	92.6	23.9	0.64	0.43
100.8	44	36	17.79	23.84	3.24	92.4	26.1	0.62	0.43
101.0	44	36	17.82	23.92	3.24	92.4	26.4	0.62	0.43
100.9	44	37	17.65	23.81	3.18	92.1	28.0	0.62	0.44
100.8	44	37	17.69	23.92	3.24	92.1	28.5	0.61	0.44
100.8	44	37	17.67	23.92	3.24	92.1	28.5	0.61	0.44
100.6	44	38	17.63	23.92	3.25	91.8	31.2	0.60	0.44
100.8	44	38	17.61	23.94	3.25	91.8	31.2	0.60	0.44
100.6	44	38	17.61	23.94	3.25	91.8	31.2	0.60	0.44

The best obtained efficiency is 96.7 % when regulation is 6.4 %, SAR is 9.5 mW/kg and maximum current density is 1.77 A/m², but the best SAR value is 0.6 mW/kg when efficiency is 91.8 %, regulation is 31.2 % and current density is 0.44 A/m². Figures 6 and 7 help to analyze the configurations that entail the best values of efficiency, regulation, SAR and current density.

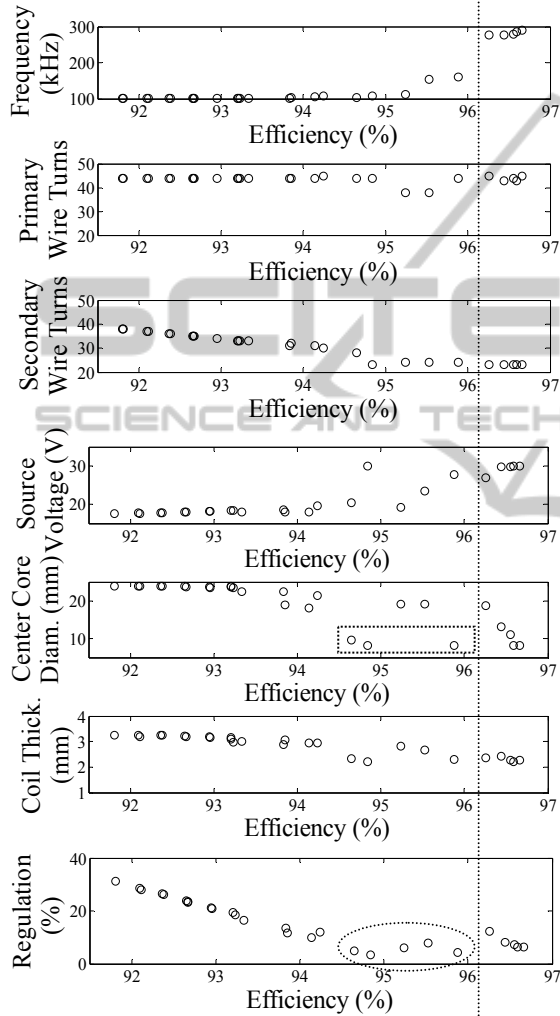


Figure 6: Value of efficiency for all the resulting configurations from MGA.

The vertical line on Figure 6 shows that the configurations on the right results in the best values of efficiency and regulation, though there are some better values of regulation on the left side, as in circled. According to this figure, for the non-dominated set of configurations, the best values of efficiency and regulation coincide when:

- The frequency is high (about 280 kHz), though the improvement of efficiency and

regulation with respect to the frequency is small after 110 kHz.

- The secondary coil has less than 28 turns.
- The source voltage is about 30 V.
- The center core diameter is smaller than 20 mm, though there are combinations with center core less than 10 mm that entail lower efficiency even with better regulation.
- The coil thickness is about 2.3 mm, though the MGA selected configurations with coil thickness between 2.22 and 3.25 mm.

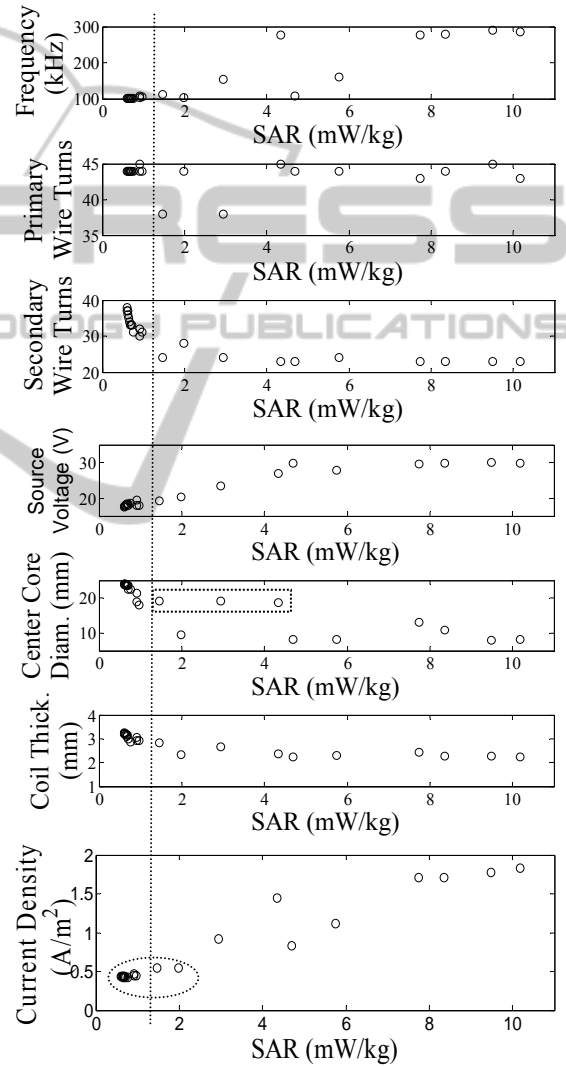


Figure 7: Value of SAR for all the resulting configurations from MGA.

Similarly, the vertical line on Figure 7 shows that the configurations on the left imply in the best values of SAR and current density. Different than for efficiency and regulation, the best values of SAR and current density coincide when:

- The frequency is about 100 kHz.
- The secondary coil has more than 30 turns.
- The source voltage is around 18 V.
- The center core diameter is bigger than 18 mm, though there are combinations with center core around 19 mm that presents higher values of SAR and current density, as shown in the square.
- The coil thickness is more than 2.8 mm.

The selected primary coil selected by MGA has between 38 and 45 turns. This parameter affects the efficiency, regulation, SAR and current density depending of the combination with the other parameters, as it can be seen on Figure 6 and 7, which show that same number of turns for the primary coil can entail good and bad values of these observed functions.

These analyses are very important at the moment of the choice of the configuration to use since the MGA returns a set with more than one non-dominated configurations. It is also important to note that even though a penalty function was added to limit the distance between the center and inside cores to make sure that the coil fits the allocated area, this might not be enough, since in the real life, it may be necessary to decrease the core center diameter even more to increase the size of the area to better allocate the coils.

5 CONCLUSIONS

A reliable model for efficiency, regulation, SAR and load power as a function of center core diameter, coil thickness, primary and secondary coil number of turns, and source voltage and frequency was created by a Kriging model that used a set of TET system configurations simulated virtually through a Flux-2D. Though the Kriging models were not supplied with the information of using serial resonant capacitors, they were acceptable with errors smaller than 15 % when compared with the finite element method calculations.

This model was used by the MGA to find a set of 32 good configurations (non-dominated set) that result in high efficiency at lower regulation and SAR with less computational cost than when using the finite element method. All the attained configurations generated tolerable values of SAR and induced current density with efficiencies between 92 and 97 % and regulations between 3.4 and 31.2 %.

An analysis of the efficiency, regulation, SAR and current density versus each of the parameters for the

resulting configurations from MGA was also performed, indicating that SAR and current density follow a similar trend. Thus, even though the current density was not taken into account in the optimization process, the minimization of SAR is a kind of indirect minimization of the current density.

The efficiency and regulation also follow the same trend, but they are contradictory to SAR and current density.

Since the resulting SAR and current density from all the configurations of the non-dominated set presented suitable values within the ICNIRP limits, the selection of better efficiency and regulation may prevail at the final choice for implementation.

REFERENCES

- Dissanavake, T. D., Hu, A. P., Malpas, S., Bennet, L., Taberner, A., Booth, L., Budgett D., 2009. Experimental Study of a TET System for Implantable Biomedical Devices. *IEEE Trans. on Biomedical Circuits and Systems*, vol. 3, no. 6.
- Joung, G. B., Cho, B. H., 1996. An Energy Transmission System for an Artificial Heart Using Leakage Inductance Compensation of Transcutaneous Transformer. *Power Electronics Specialists Conference*, vol.1, IEEE, pp. 898-904.
- Ghahary, A., Cho, B. H., 1992. Design of a Tanscutaneous Energy Transmission System using a series resonant Converter. *IEEE Transaction on Power electronics*, pp. 261-269.
- Johnson, C. C., 1975. Recommendations for specifying EM wave irradiation conditions in bioeffects research. *J. Microwave Power*, vol. 10, pp. 249-250.
- Lebensztajn, L., Marretto, C. A. R., Costa, M. C., Coulomb, J. L., 2004. Kriging: a useful tool to electromagnetic devices optimization. *IEEE Trans. on Magnetics*, v. 40, no. 2, pp. 1196-1199.
- Institute for Applied Physics Nello Carrara. *An Internet resource for the calculation of the dielectric properties of the body tissues in the frequency range 10 Hz–100 GHz*. Available at: URL:<http://niremf.ifac.cnr.it/tissprop/>.
- Vieira, D. A. G., Adriano, R. L. S., Vasconcelos, J. A., Krahenbuhl, L., 2004. Treating Constraints as Objectives in Multiobjective Optimization Problems using Niched Pareto Genetic Algorithm. *IEEE Trans. On Magnetics*, v40, no. 2, pp. 1188-1191.
- ICNIRP (International Commission on Non-Ionizing Radiation Protection), 1998 Guidelines for Limiting Exposure to Time-Varying Electric, Magnetic, and Electromagnetic Fields (up to 300 GHz). *Health Phys.*, vol. 74, no. 4, pp. 494–522.